Picosecond laser ultrasonic measurements of interlayer elastic properties of 2H-$MoSe_2$ and 2H-WSe_2

Ellis Thompson,[a] Emma Manzella, [a] Ethan Murray,[a] Madelaine Pelletier,[a] Jacob Stuligross,[a] Brian C. Daly,[a†] Seng Huat Lee,[b] Ronald Redwing[b]

a: Vassar College, 124 Raymond Ave, Poughkeepsie, NY, USA 12604

b: 2D Crystal Consortium, Materials Research Institute, Materials Research Institute, Pennsylvania State University, University Park, PA 16802, USA

†: corresponding author's email: brdaly@vassar.edu

Abstract:

We have used the ultrafast pump-probe technique known as picosecond ultrasonics to generate and detect coherent acoustic phonon pulses with frequencies reaching 40 GHz in exfoliated crystals of $MoSe_2$ and WSe_2 on Si and sapphire substrates. We report picosecond time-resolved reflectivity data from samples ranging from 180 nm to 920 nm in thickness and compare our results to a 1D simulation of strain-induced changes in the optical reflectivity. We find the longitudinal sound velocity along the *c*-axis (the interlayer direction) to be 2800 m/s ± 40 m/s for $MoSe_2$ and 2510 m/s ± 60 m/s for WSe_2. We also report the measured lifetime of longitudinal acoustic phonons approaching 40 GHz to be 0.85 ± 0.2 ns and compare this value with predictions of relaxation damping and 3-phonon models as well as discuss its relationship to the predicted thermal conductivity of $MoSe_2$.

Keywords: ultrafast optics; picosecond ultrasonics; laser ultrasonics; sound velocity; acoustic attenuation, phonon lifetime, transition metal dichalcogenides

I. Introduction

Mono- and few-layer transition metal dichalcogenides (TMDs) have become an important material for optoelectronic device applications.[1,2] In particular, the optical properties of these materials are predicted to show an enormous sensitivity to the presence of strain,[3,4,5,6,7] which would make them an ideal material for novel coherent phonon imaging schemes.[8] Furthermore, application of few-layer TMDs to nanoscale devices will depend strongly on their elastic and thermal properties which will be related to the properties of TMD bulk crystals. In this paper, we report ultrafast optical measurements of transient strain-induced reflectivity changes in bulk crystals of two TMDs: $MoSe_2$ and WSe_2. We used picosecond laser ultrasonics [9,10] (PLU) to obtain measurements of the longitudinal sound velocity along the *c*-axis (the interlayer direction) in these hexagonally structured layered crystals. Within experimental uncertainty, our results are in agreement with the few available results in the literature. By measuring the relative size of the

signals from ultrasonic pulses that have made multiple round trips in crystals ranging from 180 nm up to 920 nm, we have also measured the ultrasonic attenuation (and therefore the phonon lifetime) for ~40 GHz longitudinal acoustic phonons. Our measured phonon lifetime in $MoSe_2$ is about a factor of two lower than a previous report,[11] but it is in slightly better agreement with a 2019 molecular dynamics calculation.[12] A novel aspect of the present work is that measurements are reported from samples that were mechanically exfoliated onto planar substrates, in contrast to the more challenging arrangement of a suspended membrane.

II. Materials and Methods

PLU is an ultrafast optical pump-probe experiment that has been described extensively in the literature.[9,10] A close-up schematic of the experiment is illustrated in Fig. 1a. High-quality bulk single crystals of 2H-$MoSe_2$ and 2H-WSe_2 (2H- refers to the trigonal prismatic crystallographic phase; we hereafter omit this prefix) were synthesized by chemical vapor transport (CVT). Prior to the growth of single crystals, the $MoSe_2$ and WSe_2 polycrystalline were compounded by heating a stoichiometry mixture of pure elements at 850 ºC for three days in an evacuated, sealed quartz tube. The single crystals were grown from the synthesized polycrystalline by CVT with iodine as the transport agent at a concentration of 3.5 mg/cm^3. The growth ran for eight days in which the charge and growth zone temperatures were set to 930 ºC and 830 ºC for $MoSe_2$ and 995 ºC and 850 ºC for WSe_2, respectively. The lateral dimensions of the single crystals can range up to 5 mm x 7 mm. We then mechanically exfoliated flakes of the crystals onto Si or sapphire substrates. We performed the PLU experiment using a Ti:Sapphire oscillator operating at a 76 MHz repetition rate with degenerate pump and probe wavelengths ranging from 760 nm to 830 nm. We used a pump beam with an average power ranging from 10 – 20 mW and probe beam power ranging from 5 – 10 mW; both beams were focused to a spot size with a of 20 μm colinearly through a 5X long working distance microscope objective. The experiments were performed at room temperature and pressure. During these experiments, optical pump pulses are partially absorbed by the TMD layer, causing a rapid thermal expansion that is largest at the free surface of the TMD. This expansion launches a coherent longitudinal strain pulse composed of phonons with bandwidth and peak frequency approaching 40 GHz. As this strain pulse propagates back and forth it modifies the optical constants of the TMD and these changes are detected by measuring the reflectivity of probe pulses that are delayed by means of a mechanical stage in the probe beam arm of the experiment. Figure 1b shows ΔR for a 630 nm thick crystal of $MoSe_2$. There is initially a large reflectivity response to the arrival of the pump pulse which for these wavelengths is close to the excitonic bandgap value for these two materials. This initial response decays rapidly during the first few ps and the ΔR signal then settles into a more gradual exponential decay that represents the cooling of the lattice on the time scale of 100's of ps to a few ns. The picosecond ultrasonic signals are the oscillations centered about 450 ps and again at 900 ps, that can be most clearly seen in the inset of Fig. 1b. The 450 ps delay between those two sets of oscillations represents the time it takes the longitudinal strain pulse to make one round

Figure 1

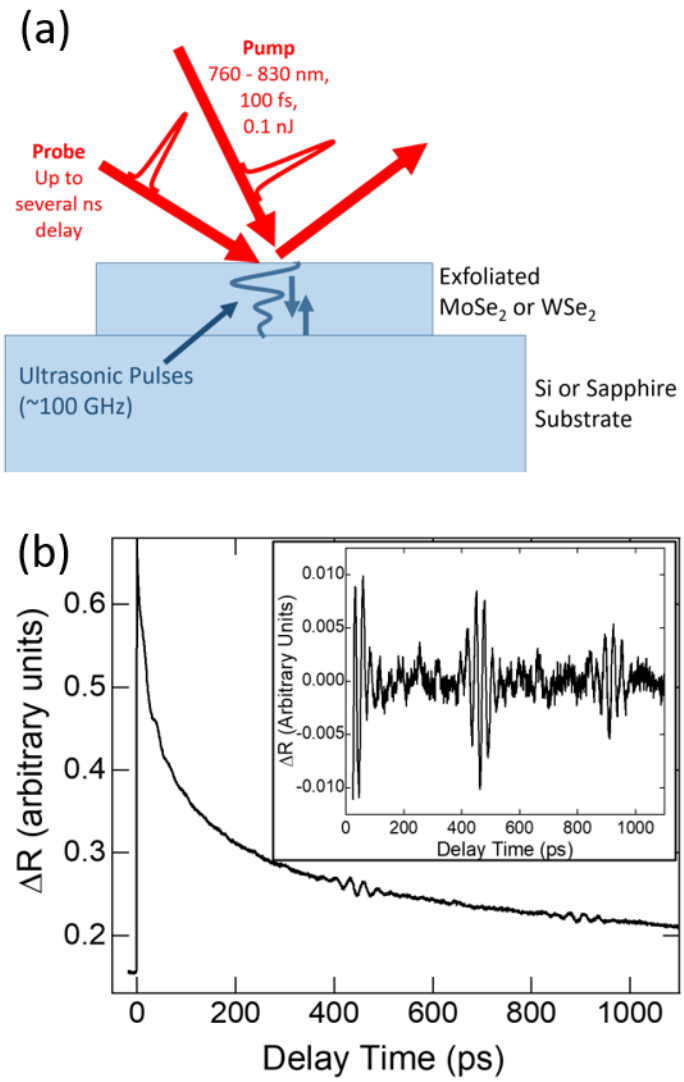

Figure 1: (a) Ultrafast pump-probe schematic. Measured exfoliated crystal thicknesses *d* ranged from 180 nm to 920 nm as measured by AFM and/or picosecond ultrasonics. (b) ΔR for 800 nm pump and 800 nm probe light for a 630 nm thick crystal of $MoSe_2$. (b, inset) ΔR for the same data with electronic and thermal response subtracted.

trip back and forth in the TMD layer. In other words, the strain pulse detected at 450 ps has traveled 1 round trip in the layer, and the strain pulse detected at 900 ps has traveled 2 round trips in the layer. In all the measurements described here, The ΔR signals such as those in the inset of Fig. 1b consist of an overall envelope and an oscillation with a Fourier spectrum that peaks in the range of 30 – 40 GHz (See Fig. 3b). This oscillating signal (sometimes called picosecond acoustic interferometry) in the ΔR is caused by the interference of the probe pulses reflected from the top surface of the TMD layer with the probe pulses reflected from the propagating strain pulse. The frequency f can be calculated from the expression

$$f = 2v_L n/\lambda \quad (1)$$

where v_L is the longitudinal sound velocity along the *c*-axis, n is the index of refraction of the TMD and λ is the wavelength of the light in vacuum. [13] In the range of wavelengths studied here, of $MoSe_2$ varies from 60 nm to 130 nm and n varies from 4.4 to 5.2.[14] For WSe_2 the optical penetration depth ranges from 60 nm up to 952 nm and n varies from 4.4 to 5.4.[15,16] This variation means that for certain wavelengths and thinner samples, a significant proportion of the optical beam intensity penetrates entirely through the sample. For each sample we varied the wavelength so that the signal-to-noise of the oscillations such as those at 450 and 900 ps in Fig. 1b was maximized while also ensuring that the consecutive signals did not overlap (note that in the top curve of Fig. 3a the signals come very close to overlapping).

III. Results and Analysis - Sound Velocity, Thickness, and Elastic Stiffness Constant

To most accurately determine sample thickness and sound velocity, we fit the experimental results to a 1-D numerical simulation of the ΔR that accounts for changes in the optical properties of the sample due to the transient strain pulse as it propagates back and forth in the sample layer.[10] An example of the simulation's capability is illustrated in Fig. 2a for comparison to 800 nm pump-probe data taken on a 350 nm WSe_2 layer exfoliated onto a Sapphire substrate. We used literature values for the optical constants and density of the sample layers but varied the thickness and sound velocity in order to obtain best fits to the data. Other properties such as the dependence of optical properties on strain and the acoustic attenuation are treated as fitting parameters. The former only modifies the sign and overall scaling factor of the simulated oscillations, while the latter affects only the relative size of each returning signal and so these do not impact the determination of the sound velocity. A compliant 3 – 5 nm layer is also added between the Si and the $MoSe_2$ in order to represent the native Si oxide and the weak Van der Waals interfacial bonding and this also affects the relative size of each returning signal. While the time duration between each returning round-trip signal depends primarily on v_L and sample thickness d, the simulations provide enough information to independently obtain v_L and d. Furthermore, for one WSe_2 sample and one $MoSe_2$ sample, we have compared our measurements of d obtained this way with AFM measurements and found our results to be in agreement within

Figure 2

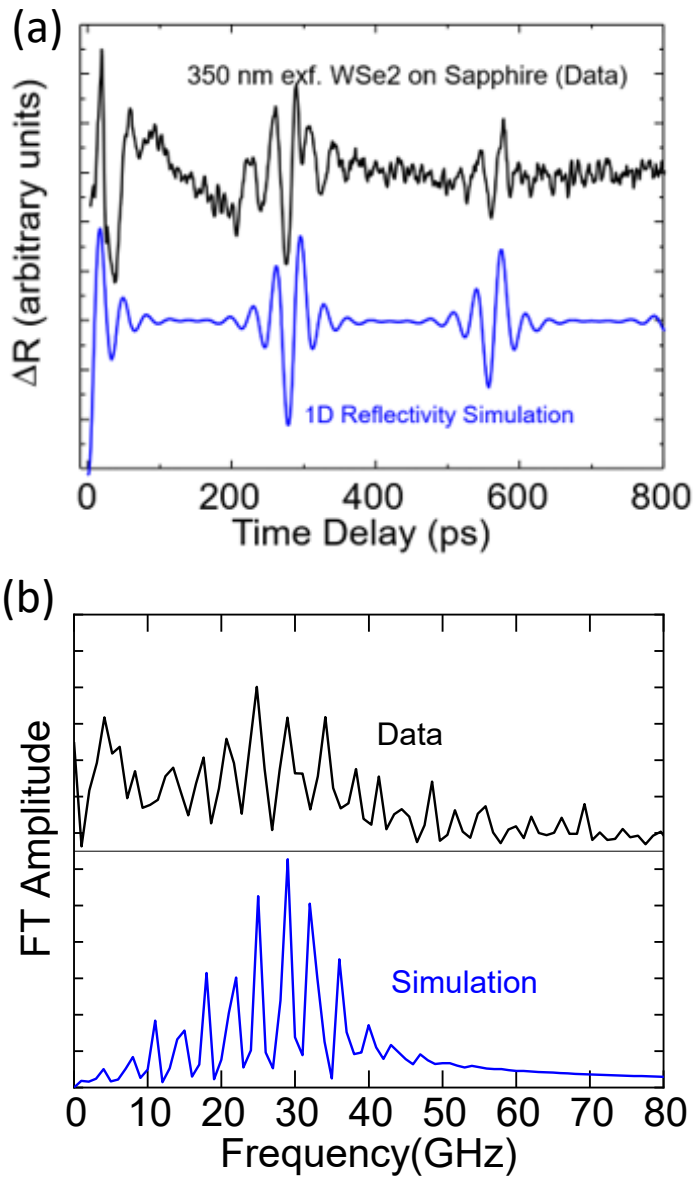

Figure 2: (a) PLU data and 1-D simulation for a 350 nm WSe_2 sample. For this simulation v_L =2510 m/s, the attenuation factor was $0.02\times\omega^2$ in units of ps (equivalent to 5000 cm^{-1} at 40 GHz), and a 3 nm compliant interface layer with v_L =2700 m/s and ρ = 1.1 g cm^{-3} (b) Fourier transform of the data and simulation in (a).

5%. In Fig. 2b, we compare the Fourier transforms of the reflectivity data and simulation. The frequency comb behavior observed here is expected for free-standing membranes and is discussed in more detail in Sec. IV. While the simulated spectrum correctly reproduces the general features of the data spectrum, it is clear that the simulation fails to account for some of the lowest and highest frequencies observed in the data. Barring any experimental anomalies, this may indicate the limitations of using the simple ω^2–dependent attenuation that we implement our 1D simulations. We discuss attenuation more in detail in Sec. IV.

Based on measurements from three samples of WSe_2 and five samples of $MoSe_2$, we find the longitudinal sound velocity along the *c*-axis of crystalline $MoSe_2$ to be 2800 m/s ± 40 m/s and WSe_2 to be 2510 m/s ± 60 m/s. These correspond to values of the elastic stiffness constant C_{33} = 54.0 ± 1.5 GPa for $MoSe_2$ and C_{33} = 58.7 ± 2.8 GPa for WSe_2. A review of the literature does not yield many reports of these material properties. Our measured values are, however, comparable to two published results on thin layers: A Raman measurement of C_{33} on few-layer WSe_2 in 2013 yielded a result of 52.1 GPa – roughly 10% below our measurement,[17] and a 2019 report on ultrafast optical measurements of resonant frequencies of free standing $MoSe_2$ membranes found a longitudinal sound velocity along the *c*-axis of 2820 m/s.[11] These relatively low values for sound speed and elastic constant along the *c*-axis (relative to those along the *a*-axis) are expected in TMD materials due to the weak Van der Waal's bonding in that direction.[18,19,20,21]

IV. Results and Analysis: Frequency Domain and Phonon Attenuation

Since our experiment gives us access to multiple ultrasonic signals traveling back and forth in crystals of varying thickness, it is possible to obtain a measurement of the attenuation of phonons approaching 40 GHz. We followed the techniques described in two previous studies of crystalline and amorphous silicon,[22,23] using measurements such as the ones shown in Fig. 3a to determine the attenuation of longitudinal acoustic phonons along the *c*-axis in $MoSe_2$. The top curve of Fig. 3a is from data taken on a 350 nm thick sample of $MoSe_2$, and shows five distinctly separate $\Delta R(t)$ signals from acoustic phonon pulses spaced roughly 200 ps apart after the initial signal near time zero. Each successive signal is reduced compared to its predecessor due to a combination of surface/interface losses and intrinsic losses in the bulk of the sample layer. The 920 nm thick sample shows only two returning signals in this same range of pump-probe time delay. Figure 3b shows the Fourier transform amplitude of the two signals from the 920 nm thick layer of $MoSe_2$, which shows measurable components approaching 40 GHz.

In addition to examining the Fourier spectra of the individual transients as in Fig. 3b, we also plot the Fourier spectra of the entire ΔR versus delay time signal for the 350 nm and 920 nm thick $MoSe_2$ in Fig. 4. These spectra take the form of a frequency comb with components for the 920 nm layer. These frequency spacings are approximately equal to $\left(2d/v_L\right)^{-1}$ which are

Figure 3

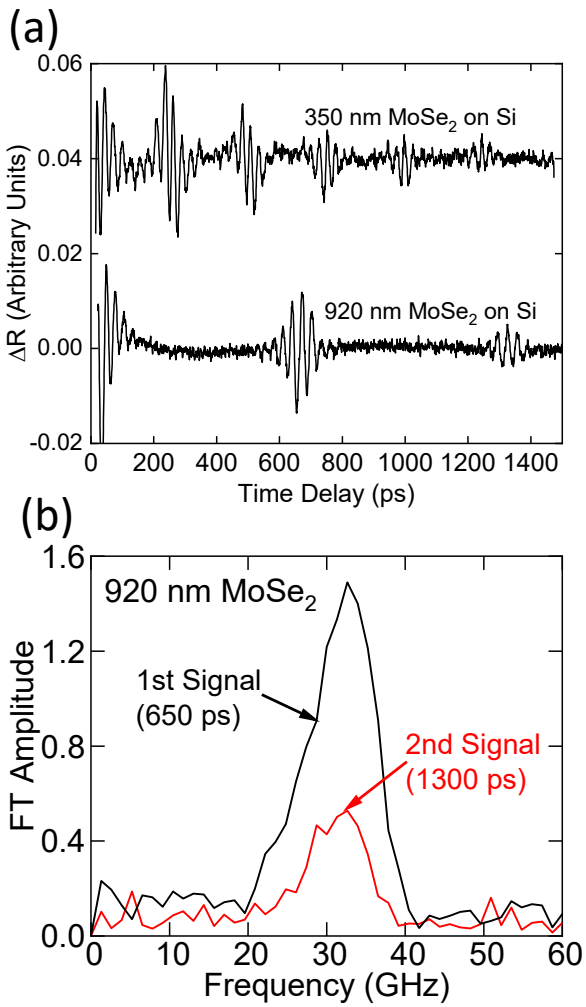

Figure 3: (a) ΔR for two $MoSe_2$ samples with d =350 nm and 920 nm. 5 oscillatory signals each separated by ~ 200 ps are visible for the thinner sample, while 2 signals separated by ~ 650 ps are visible for the thicker sample. (b) Fourier transform of the individual transient signals at 650 ps and 1300 ps in the lower curve of (a).

Figure 4

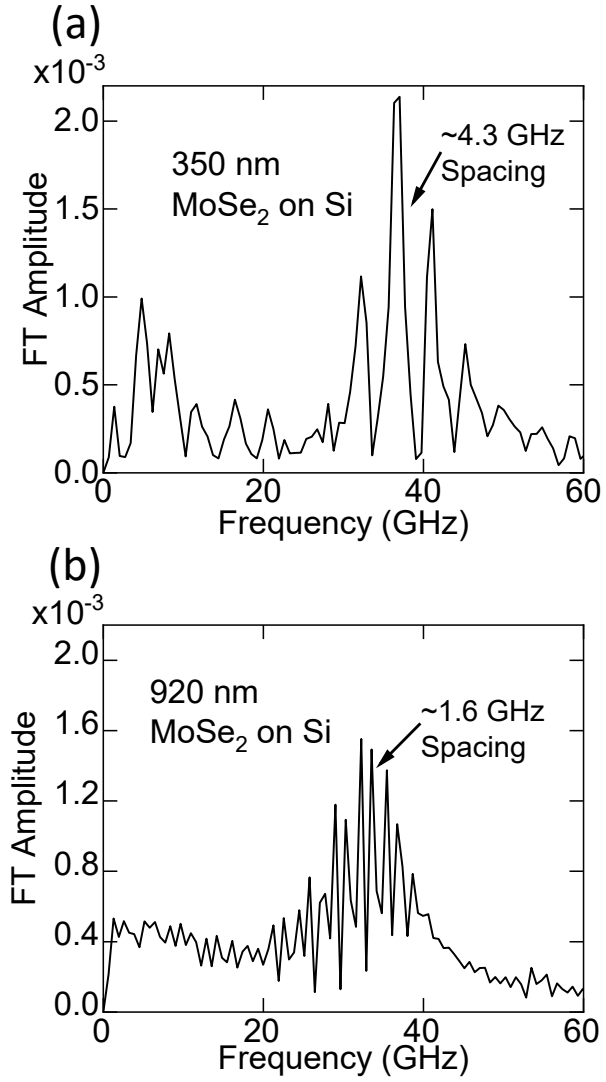

Figure 4: Fourier transforms of the data in Fig. 3a. (a) Frequency comb spacing is ~ 4.3 GHz for the 350 nm $MoSe_2$ layer. (b) Frequency comb spacing is ~1.6 GHz for the 920 nm $MoSe_2$ layer.

reaching beyond 40 GHz that are evenly spaced by ~4.3 GHz for the 350 nm layer and ~1.6 GHz for the resonant frequencies of a free-standing layer. This frequency comb behavior has been previously observed in picosecond laser ultrasonic measurements on free-standing membranes of Al coated Si[24] and is also reported in the studies of free standing $MoSe_2$ of Ref. 11. The fact that we observe this frequency comb behavior in samples that were mechanically exfoliated onto a planar substrate is indicative of weak sample-substrate bonding. To obtain a value for the attenuation α for the ~40 GHz phonons we compare the changes in the peak-to-peak amplitudes of successive $\Delta R(t)$ signals using the relationship

$$\alpha = \frac{1}{2d}\ln\left(\frac{r\Delta R_n}{\Delta R_{n+1}}\right) \tag{2}$$

where ΔR_n is the nth signal from a phonon pulse that has made n round trips in the sample and r is a factor that represents the amount of phonon signal that is lost upon reflection at the interfaces of the sample. In Fig. 5 we plot the ratio $\Delta R_n/\Delta R_{n+1}$ for 5 different $MoSe_2$ samples of varying thickness exfoliated onto Si. For the thicker samples such as the 920 nm sample (lower curve of Fig. 3a), only the signal ratio $\Delta R_2/\Delta R_1$ could be used, but for the thinner samples signal ratios up through $\Delta R_5/\Delta R_4$ were available, reducing the measurements' uncertainties. Reflection and interface losses are determined by noting that for the three thinnest samples, the signal ratios are effectively the same within the margin of uncertainty of the experiment. This average is indicated by the blue dashed horizontal line at $\Delta R_n/\Delta R_{n+1} = 1.90$. The value of the experimentally determined reflection coefficient r to be used in Eq. (2) is determined by taking the inverse of this number, in this case $r = 0.53$. If we had a well-bonded interface between $MoSe_2$ and Si we would expect this reflection coefficient to be given by an acoustic mismatch calculation

$$r = \left(\rho_{Si}v_{L,Si} - \rho_{MoSe_2}v_{L,MoSe_2}\right)\Big/\left(\rho_{Si}v_{L,Si} + \rho_{MoSe_2}v_{L,MoSe_2}\right) \tag{3}$$

where using the accepted literature values $\rho_{Si} = 2.3\,g\,cm^{-3}, \rho_{MoSe_2} = 6.9\,g\,cm^{-3}, v_{L,Si} = 8400\,m\,s^{-1}$, along with $v_{L,MoSe_2} = 2800\ m\ s^{-1}$ as reported in this work coincidentally yields a value of $r = 0$. The two materials are elastically very well-matched, though it should be noted that the silicon native oxide layer would be somewhat more compliant than the Si. Our experimental value of r is another indicator of the weak nature of the bonding that occurs in a mechanical exfoliation onto an Si wafer. A 2016 picosecond ultrasonic study of InSe on Sapphire found a similar effect – the high frequency ultrasonic behavior of thin flakes mechanically exfoliated onto substrates is more akin to that of a free-standing layer than that of an ideal elastic interface.[25] The fact that r is not equal to unity as would be the case for an ideal free standing layer is due to multiple

Figure 5

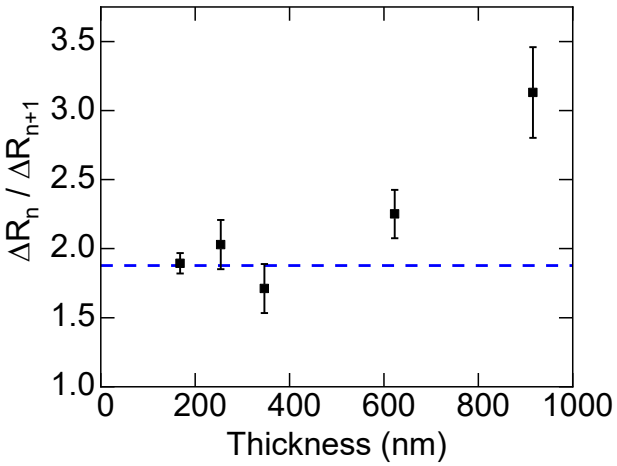

Figure 5: Averaged value of $\Delta R_n / \Delta R_{n+1}$ (■) for the ~40 GHz phonon pulses for five $MoSe_2$ samples of varying thickness. The reflection and interface losses are determined experimentally and are indicated by the dashed line at 1.90. All loss above this line is considered to be intrinsic to the $MoSe_2$.

factors including the limited transmission of some acoustic energy into the Si through the weak Van der Waal's bonding and the native silicon oxide, scattering of acoustic energy due to roughness of the mechanically exfoliated layers, and losses due to thickness variation over the 20 μm optical spot size.

Employing Eq. 2 using the values of $\Delta R_2/\Delta R_1$ for the two thicker samples yields a measurement of the attenuation α of 2100 ± 670 cm^{-1} for these longitudinal ultrasonic pulses. This is over 20 times higher than the attenuation of 50 GHz longitudinal ultrasound in [100] Si reported in Ref. 22. From the relationship $\tau = \left(2\alpha v_L\right)^{-1}$ we find the phonon lifetime τ for ~ 40 GHz longitudinal acoustic phonons to be 0.85 ± 0.2 ns. This measured lifetime is a factor of two lower than was reported in Ref. 11 for 40 GHz LA phonons resonating in a 54-layer suspended membrane of 2H-$MoSe_2$. A 2019 molecular dynamics study of phonon lifetimes and thermal conductivity in TMD materials predicted a lifetime for the longest wavelength phonons that is in closer agreement with our measurement.[12] The supplemental material for Ref. 12 reports lifetimes of 0.4 ns – 0.8 ns for acoustic phonons with frequency less than 150 GHz in $MoSe_2$.

A rigorous analysis of the lifetime of long wavelength phonons in the range of 10 GHz to a few 100 GHz is often challenging due to the sparse amount of data available and the applicability of two distinct models that are well-described in the literature. The first of these models is a Landau-Rumer approach that describes a fully quantum mechanical three-phonon scattering process in which the long wavelength phonon of interest is the lowest frequency phonon in a collision involving two higher frequency phonons.[26] The second is a relaxation damping or Akhieser approach where the long wavelength phonon of interest disturbs the overall thermal phonon population which then removes energy from the long wavelength mode as it returns to thermal equilibrium.[27,28] The first approach is considered ideal for frequencies such that $\omega\tau_{TH} > 1$ while the second approach, originally envisioned as an explanation for ultrasound attenuation in the 10 MHz – 1 GHz range, is expected to be most applicable for $\omega\tau_{TH} < 1$. However, here considering ~40 GHz phonons in a material with typical thermal phonon lifetimes ranging from 1-2 ps at optical phonon frequencies up to typical values of 100 ps at acoustic phonon frequencies,[12] an intermediate range of $\omega\tau_{TH} = 0.2 - 20$ can be expected.

A detailed 3-phonon calculation employing the single-mode relaxation time (SMRT) approximation and which also accounts for the strong elastic anisotropy in $MoSe_2$ is presented in Ref. 11 and its supplementary materials. The one variable parameter in this 3-phonon model is the average Gruneisen parameter γ and by fitting their experimental data on resonant modes in suspended flakes of $MoSe_2$ they found a best value of γ = 1.8, which can be compared with a predicted value of 1.2 calculated by density functional theory.[29] However, given that our

measured lifetime is half of that reported in Ref. 11, and the fact that the lifetime τ of our long wavelength phonon is proportional to γ^{-2}, then a similar calculation for our result would require $\gamma = 2.5$ which would be somewhat large for this constant that reliably remains near 1 for most materials.

The relaxation damping approach predicts a lifetime for the long wavelength phonon given by[11,22,27]

$$\tau^{-1} = \frac{CT}{\rho v_L^{\,2}} \frac{\omega^2 \tau_{TH}}{1+\omega^2 \tau_{TH}^{\,2}} \gamma^2 \qquad (4)$$

where C is the volumetric heat capacity (1.87×10^6 J m^{-3} K^{-1}) and T is 300 K. To find τ_{TH} we can use the kinetic formula for thermal conductivity $\kappa = C v_{AV}^{\,2} \tau_{TH} / 3$. Here $v_{AV} = 3220$ m s^{-1} is a phonon velocity (see supplemental materials of Ref. 11) averaged over the TA and LA modes as well as averaged over the highly elastically anisotropic hexagonal crystal structure. The kinetic formula can then be used to determine a value for τ_{TH}. With no measurements of κ for $MoSe_2$ available in the literature we can rely on the range of predictions 18 W m^{-1} K^{-1} – 60 W m^{-1} K^{-1} from various calculations[12,29,30] which give a range for τ_{TH} of 3 ps – 9 ps. If we employ the lowest value of $\tau_{TH} = 3$ ps in Eq. 4 we find $\gamma = 1.7$ would yield our measured lifetime for ~40 GHz phonons of 0.85 ns, but using $\tau_{TH} = 9$ ps we find $\gamma = 1.35$. This Gruneisen constant value closer to unity gives us increased confidence in the higher end of the room temperature thermal conductivity and thermal phonon lifetime predictions. It also lends support to the relaxation damping approach as opposed to the 3-phonon approach for determining the lifetime of such long wavelength phonons.

V. Summary

In summary, we have used the ultrafast optical technique of picosecond ultrasonics to measure the sound velocity and C_{33} of WSe_2 and $MoSe_2$, and the lifetime of ~40 GHz longitudinal acoustic phonons along the *c*-axis of $MoSe_2$. While we did not make measurements directly on mono- or few-layer samples, our results can be used to predict the thermal and vibrational behavior of devices constructed from monolayer versions of these materials. Our technique is relatively simple compared to techniques that rely on free standing samples, as our samples were simply exfoliated onto planar substrates.

Acknowledgements

The authors acknowledge the support of National Science Foundation award number DMR-1709521 "RUI: Acoustic Phonons in Nanostructures: Surface Waves, Thermal Transport, and

Imaging." This study is based upon research conducted at The Pennsylvania State University Two-Dimensional Crystal Consortium – Materials Innovation Platform (2DCC-MIP) which is supported by NSF cooperative agreement DMR-1539916.

Author Contributions

Ellis Thompson: Investigation, Formal analysis, Visualization, **Emma Manzella:** Software, Writing-Review and Editing **Ethan Murray:** Investigation **Madelaine Pelletier:** Resources **Jacob Stuligross:** Software, Formal analysis, Writing-Review and Editing **Brian Daly:** Writing-Original Draft, Conceptualization, Supervision, Visualization, Formal Analysis **Seng-Huat Lee:** Resources, Writing-Review and Editing **Ronald Redwing:** Resources, Supervision

Data Availability

The raw/processed data required to reproduce these findings cannot be shared at this time due to technical or time limitations. Please email Brian Daly brdaly@vassar.edu to obtain any raw data files related to this manuscript.

References

[1] Q.H. Wang, K. Kalantar-Zadeh, A. Kis, J.N. Coleman, and M.S. Strano, Electronics and optoelectronics of two-dimensional transition metal dichalcogenides, Nature Nanotech. 7 (2012) 699-712.

[2] K.F. Mak and J. Shan, Photonics and optoelectronics of 2D semiconductor transition metal dichalcogenides, Nature Photonics 10 (2016) 216-226.

[3] A. Steinhoff, M. Rosner, F. Jahnke, T.O. Wehling, and C. Gies, Influence of excited carriers on the optical properties of MoS_2, Nano Lett. 14 (2014) 3743-3748.

[4] S.B. Desai et. al.,Strain-induced indirect to direct bandgap transition in multilayer WSe_2, Nano Lett. 14 (2014) 4592-4597.

[5] O.B. Aslan, M. Deng, and T.F. Heinz, Strain tuning of excitons in monolayer WSe_2, Phys. Rev. B 98 (2018) 115308.

[6] S. Aas and C. Bulutay, Strain dependence of photoluminescence and circular dichroism in transition metal dichalcogenides: a k·p analysis, Optics Express 26 (2018) 340519.

[7] M. Feierabend, A. Morlet, G. Berghauser, and E. Malic, Impact of strain on the optical fingerprint of monolayer transition metal dichalcogenides, Phys. Rev. B 96 (2017) 045425.

[8] B.C. Daly et al., Imaging nanostructures with coherent phonon pulses, Appl. Phys. Lett. 84 (2004) 5180-5182.

[9] G. A. Antonelli, B. Perrin, B. C. Daly, and D. G. Cahill, Characterization of Mechanical and Thermal Properties Using Ultrafast Optical Metrology, MRS Bull. 31 (2006) 607-613.

[10] C. Thomsen, H. T. Grahn, H. J. Maris, and J. Tauc, Surface generation and detection of phonons by picosecond light pulses, Phys. Rev. B 34 (1986) 4129-4138.

[11] P. Soubelet, A.A. Reynoso, A. Fainstein, K. Nogajewski, M. Potemski, C. Faugeras, and A.E. Bruchhausen. The lifetime of interlayer breathing modes of few-layer 2H-$MoSe_2$ membranes, Nanoscale 11 (2019) 10446-10453.

[12] A. Mobraki, C. Sevik, H. Yapicioglu, D. Cakir, and O. Gulseren, Temperature-dependent phonon spectrum of transition metal dichalcogenides calculated from the spectral energy density: Lattice thermal conductivity as an application, Phys. Rev. B 100 (2019) 035402.

[13] H.-N. Lin, R.J. Stoner, H.J. Maris, and J. Tauc, Phonon attenuation and velocity measurements in transparent materials by picosecond acoustic interferometry, J. Appl. Phys. 69 (1991) 3816-3822.

[14] A. R. Beal and H. P. Huges, Kramers-Kronig analysis of the reflectivity spectra of 2H-MoS2, 2H-MoSe2, and 2H-MoTe2, J. Phys. C 12 (1979) 881.

[15] A.R. Beal, W.Y. Liang, and H.P. Huges, Kramers-Kronig analysis of the reflectivity spectra of 3R-WS2 and 2H-WSe2, J. Phys. C 9 (1976) 2449-2457.

[16] C. Hsu et. al., Thickness-Dependent Refractive Index of 1L, 2L, and 3L MoS2, MoSe2, WS2, and WSe2, Adv. Opt. Mater. 7 (2019) 1900239.

[17] Y. Zhao et. al., Interlayer Breathing and Shear Modes in Few-Trilayer MoS_2 and WSe_2, Nano Lett. 13 (2013) 1007-1015.

[18] N. Wakabayashi, H. G. Smith, and R. M. Nicklow, Lattice dynamics of hexagonal MoS_2 studied by neutron scattering, Phys. Rev. B 12 (1975) 659-663.

[19] C. Chiritescu, D. G. Cahill, N. Nguyen, D. Johnson, A. Bodapati, P. Keblinski, and P. Zschack, Ultralow Thermal Conductivity in Disordered, Layered WSe2 Crystals, Science 315 (2007) 351-353.

[20] C. Muratore et. al., Cross-plane thermal properties of transition metal dichalcogenides, Appl. Phys. Lett. 102 (2013) 081604.

[21] J.L. Feldman, Elastic Constants of 2H-MoS_2 and 2H-NbSe Extracted from Measured Dispersion Curves and Linear Compressibilities, J. Phys. Chem. Solids 37 (1976) 1141-1144.

[22] B.C. Daly, K. Kang, Y. Wang, and D.G. Cahill, Picosecond ultrasonic measurements of attenuation of longitudinal acoustic phonons in silicon, Phys. Rev. B 80 (2009) 174112.

[23] D.B. Hondongwa, B.C. Daly, T.B. Norris, B. Yan, J. Yang, and S. Guha, Ultrasonic attenuation in amorphous silicon at 50 and 100 GHz, Phys. Rev. B 83 (2011) 121303R.

[24] M. Grossman et. al., Femtosecond spectroscopy of acoustic frequency combs in the 100-GHz frequency range in Al/Si membranes, Phys. Rev. B 88 (2013) 205202.

[25] R. Beardley et. al., Nanomechanical probing of the layer/substrate interface of an exfoliated InSe sheet on sapphire, Sci. Rep. 6 (2016) 26970.

[26] G. P. Srivastava, The Physics of Phonons, Adam Hilger, NY, 1st Ed. 1990.

[27] H. J. Maris, Interaction of sound waves with thermal phonons in crystals, in: W.P. Mason and R.N. Thurston (Eds.), Physical Acoustics, Academic Press, New York (1971) 279-336.

[28] R. Truell, C. Elbaum, and B.B. Chick, Ultrasonic Methods in Solid State Physics, Academic Press, New York, 1st Ed. 1969.

[29] B. Peng, H. Zhang, H. Shao, Y. Xu, X. Zhang, and H. Zhu, Thermal conductivity of monolayer MoS_2, $MoSe_2$, and WS_2: interplay of mass effect, interatomic bonding and anharmonicity, R. Soc. Chem. Adv. 6 (2016) 5767-5773.

[30] M. Zulfiqar, Y. Zhao, G. Li, Z.-C. Li, and J. Ni, Intrinsic Thermal conductivities of monolayer transition metal dichalcogenides MX_2 (M = Mo, W; X = S, Se, Te), Sci. Rep. 9 (2019) 4571.

Figure Captions

Figure 1: (a) Ultrafast pump-probe schematic. Measured exfoliated crystal thicknesses *d* ranged from 180 nm to 920 nm as measured by AFM and/or picosecond ultrasonics. (b) ΔR for 800 nm pump and probe light for a 630 nm thick crystal of $MoSe_2$. (b, inset) ΔR for the same data with electronic and thermal response subtracted.

Figure 2: (a) PLU data and 1-D simulation for a 350 nm WSe_2 sample. Simulation sound velocity is 2510 m/s. (b) Fourier transform of the data and simulation in (a).

Figure 3: (a) ΔR for two $MoSe_2$ samples with d =350 nm and 920 nm. 5 oscillatory signals each separated by ~ 200 ps are visible for the thinner sample, while 2 signals separated by ~ 650 ps are visible for the thicker sample. (b) Fourier transform of the individual transient signals at 650 ps and 1300 ps in the lower curve of (a).

Figure 4: Fourier transforms of the data in Fig. 3a. (a) Frequency comb spacing is ~ 4.3 GHz for the 350 nm $MoSe_2$ layer. (b) Frequency comb spacing is ~1.6 GHz for the 920 nm $MoSe_2$ layer.

Figure 5: Averaged value of $\Delta R_n / \Delta R_{n+1}$ (■) for the ~40 GHz phonon pulses for five $MoSe_2$ samples of varying thickness. The reflection and interface losses are determined experimentally and are indicated by the dashed line at 1.90. All loss above this line is considered to be intrinsic to the $MoSe_2$.